Testing the Sticky Rouse Model for Polyelectrolyte Complex Coacervates

by

Frances J. Morin

B.S., College of William and Mary, 2016

Submitted to the Graduate Faculty of

the Dietrich School of Arts and Sciences in partial fulfillment

of the requirements for the degree of

Master of Science

University of Pittsburgh

2019

UNIVERSITY OF PITTSBURGH

DIETRICH SCHOOL OF ARTS AND SCIENCES

This thesis was presented

by

Frances J. Morin

It was defended on

August 2, 2019

and approved by

Jennifer Laaser, Department of Chemistry

Tara Meyer, Department of Chemistry

Geoffrey Hutchison, Department of Chemistry

Thesis Advisor: Jennifer Laaser, Department of Chemistry

Testing the Sticky Rouse Model for Polyelectrolyte Complex Coacervates

Frances J. Morin, M.S.

University of Pittsburgh, 2019

Polyelectrolyte complexes are entropically driven associations of charged macromolecules in aqueous salt solution.[1] These polyelectrolyte complexes can undergo liquid-liquid phase separation into a polymer poor supernatant and a polymer rich coacervate, which possess practical viscoelastic properties that make them valuable for product design.[2,3] With a unique salt-addition methodology, we are able to independently investigate the impact of salt concentration and polymer volume fraction on the viscoelastic properties of these materials. This allows us to independently determine the dependence of relaxation times on both variables with no approximations expanding our understanding of these dynamic materials. We find the relaxation times scales as the polymer concentration to the power of 5.82 ± 0.54 and salt concentration to the power of 1.79 ± 0.24. These values suggest that the current literature underestimates the impact of the polymer volume fraction on the viscoelastic response of polyelectrolyte complex coacervates. Furthermore, the charge density of these materials was probed with a carefully synthesized weak polyelectrolyte system in order to investigate the cooperativity of charge sites. Preliminary results suggest that this area of study will provide a deeper understanding of the driving forces behind these dynamics.

Table of Contents

1.0 Introduction 1

1.1 Phase Behavior of Polyelectrolyte Complexes 1

1.1.1 The Voorn-Overbeek Theory and Experimental Support 2

1.1.2 Theoretical and Experimental Results of Modern Coacervate Phase Behavior 4

1.2 Viscoelasticity of Complex Coacervates 4

1.2.1 Support of the Sticky Rouse Model 5

1.2.2 Failings of the Sticky Rouse Model 7

2.0 Salt-Addition Experiment 8

2.1 Introduction 8

2.2 Experimental Design 9

2.2.1 Materials 9

2.2.2 Preparation of Polyelectrolyte Complexes 9

2.2.3 Thermogravimetric Analysis 10

2.2.4 Rheological Measurements 10

2.3 Results 11

2.3.1 TGA Results 11

2.3.2 Rheological Data 13

2.4 Discussion 20

2.5 Acknowledgements 21

3.0 Charge Density Experiment 22

3.1 Introduction 22

3.2 Experimental Design 23

3.2.1 Polymer synthesis 23

3.2.1.1 Materials 23

3.2.1.2 Synthesis of Poly(acrylic acid) 23

3.2.1.3 Synthesis of Poly(dimethyl amino ethyl methacrylate-*co*-diethylene glycol methyl ether methacrylate) 25
3.2.2 Preparation of Polyelectrolyte Complexes 28
3.2.3 Rheological Measurements 28
3.3 Results and Conclusions 28
Appendix. Supporting Information for: Charge Density Experiment 34
Bibliography 37

List of Tables

1 Poly(acrylic acid) used in preliminary experiments 25
2 Poly(DMAEMA-*co*-DEGMA) used in preliminary experiments 27

List of Figures

1 Schematic of a polyelectrolyte complex phase diagram 3
2 TGA trace of the 1.4 M KBr coacervate sample. 11
3 Phase diagram for the salt-addition experiment 12
4 Raw rheology data for the series of samples with starting salt concentration of 1.4 M 14
5 Raw rheology data for the series of samples with target salt concentration of 1.8 M 15
6 Horizontal shift factors versus salt volume fraction 17
7 Fit of the relaxation time as a function of salt concentration from Fig. 6 . . . 18
8 Fit for the relaxation time as a function of polymer volume fraction 19
9 Reaction scheme: synthesis of poly(acrylic acid). 24
10 Reaction scheme: synthesis of poly(DMAEMA-*co*-DEGMA). 26
11 Reaction scheme: removal of trithiocarbonate end-group. 27
12 Raw rheology data for 100% poly(DMAEMA) and 5:1 poly(DMAEMA-*co*-DEGMA coacervates made with poly(acrylic acid) 29
13 Master curve of rheology data for poly(DMAEMA) and poly(acrylic acid) . . 30
14 Horizontal shift factors dependence on charge density for poly(DMAEMA)/poly-(acrylic acid) system 30
15 Pictures of the polymer volume fraction in coacervates with different charge densities 32
16 Rheology data illustrating reproducibility problems in weak polyelectrolyte systems 33
17 NMR data for the 5:1 poly(DMAEMA-*co*-DEGMA) after end group removal. 35
18 NMR data showing the removal of the *tert*-butyl group. 36

I'd like to begin by thanking Jennifer Laaser for all her help, patience, tough love and support during both the research and writing phase of this work. I cannot imagine working with a smarter or more admirable teacher. Your dedication to both science and teaching has inspired me to pursue education and remember that science can, and should, be fun. I'd also like to thank my committee, Dr. Tara Meyer and Dr. Geoff Hutchison for their continued support.

Each of my labmates deserves my unending gratitude for helping me through this, whether it was letting me into the optics lab when I forgot my ID or coming in on a Saturday so I could finish a synthesis. I'd like to begin by thanking Zijian Huo for sticking with me through the physical chemistry classes and helping me figure out the rheometer. I will always remember optics bay 2 fondly and I appreciate everything you've taught me. I'd like to thank Jun Huang for all the help in the coacervates trenches for three years. I definitely could not have handled this on my own. I'd like to thank Paige Moncure for being the only officemate a girl could want. For Swati, I'll miss your ASAP orders and awesome music. I want to thank you for your patience explaining organic chemistry very slowly to me. I'd also like to thank Victoria Kong for being an honest and passionate member of the lab. Watching you grow into a confident polymer physicist has been very enjoyable. Lexi Knight, I'd like to thank you for your enthusiasm in lab, your willingness to do every task with vigor and excitement is refreshing. Most importantly, I would like to thank Marissa Puppo for everything she's done for me and this project. She's been such a strong friend and scientist on this project from the beginning and I could not have managed without her. Having someone like her on the project not only made it enjoyable but made it possible. She deserves the credit for a lot of the research presented here as she developed majority of the sample preparation experiments and helped me keep a level head when things were not working and when they were.

Last of all, I'd like to thank Christoffer Friend for forcing me to stick with it through all this and being supportive of me the whole time. I'd like to thank my family for also supporting my decisions and dreams (and the occasional edits and advice) thanks Mom and Dad.

1.0 Introduction

Polyelectrolyte complexes are aqueous solutions of charged polymers that undergo liquid-liquid phase separation to form a polymer-poor supernatant and polymer-rich coacervate phase.[3] This entropically driven phase separation occurs due to the association of oppositely charged sites on the polymer chains and release of salt counter-ions. The polymer-rich coacervate phase has unique viscoelastic properties, making it a valuable area of research since the discovery of these materials in the early 19$^{\text{th}}$ century. A substantial amount of research has been done to understand how the chemistry of the charged species, effects of pH, salt or other solution changes impact the viscoelasticity of the bulk phase but important questions remain, particularly about the interplay of these factors.[4–9] These coacervates possess tunable viscoelastic properties, making them viable biomemetic tools,[10–13] underwater adhesives,[14–17] or medical imagining and drug delivery materials.[18–21]

1.1 Phase Behavior of Polyelectrolyte Complexes

In salt solutions, polyelectrolyte complexes can phase separate into a supernatant phase and a coacervate phase. As shown in Fig. 1, the phase window is a boundary under which the sample separates into two phases, a supernatant and a coacervate, and above which remains one phase. Tie-lines passing through each initial composition intersect with the phase boundary at the generated supernatant and coacervate composition. Understanding phase behavior is necessary for understanding physical properties of complex coacervates such as viscoelasticity due to the dependence of these properties on both polymer and salt volume fraction. Studies of the phase window associated with polyelectrolyte complexes show that the phase behavior depends on the polyelectrolyte pair, salt concentration and type and charge density.[6,22] The Voorn-Overbeek theory is the seminal theoretical work on polyelectolyte complex phase behavior and has successfully predicted experimental phase behavior.[23] However, more recent work suggest this theory may omit key variables, detailed

below.

1.1.1 The Voorn-Overbeek Theory and Experimental Support

Overbeek and Voorn developed a mathematical approach to model complex coacervate phase behavior. This model is based on the Flory-Huggins theory for polymer solutions but replaces the enthalpic term with a Debye-Huckel approximation for the ion energies.[23–26] This theoretical model has been successfully used for years to predict polyelectrolyte phase behavior and there is a large amount of experimental research supporting the model. For example, Spruijt *et al.* performed fluorescent measurements on fluorescently labeled polyelectrolyte complexes to determine the composition of the coacervate phase and critical salt concentration. They found solid quantitative agreement between experimental results and the Voorn-Overbeek model.[27] Priftis *et al.* tested the viscoleasticity and phase behavior of a ternary polyelectrolyte complex system. The addition of a third component had dramatic effects on the behavior including much higher tolerance for salt addition and pH changes. These changes in phase behavior were well-predicted with an adaption of the classic Voorn-Overbeek model.[28] The Larson group tested the limit of the Voorn-Overbeek theory by comparing the classic model to experimental data at a wider range of pH, salt, and chain length values. They found good experimental agreement with the Voorn-Overbeek theory, but noted that the theory had difficulty providing valid experimental predictions at high and low pH due to asymmetric association behavior between the polyanions and polycations.[29]

Despite these successes, Voorn-Overbeek omits several physically-important contributions due to the approximations made in the Debye-Huckel electrostatic term. The Debye-Huckel approximation assumes that the ions in solution are significantly diluted which is not accurate for the high salt concentrations in most coacervates. It also ignores connectivity in polymer chains, treating salt and polyions as identical.[30] Despite these limitations, there is substantial experimental agreement that allows the Voorn-Overbeek model to be used frequently, under current conditions. However, the difficulty fitting the more complex systems drove the development of the modern theory of complex coacervation described in the next section.[31]

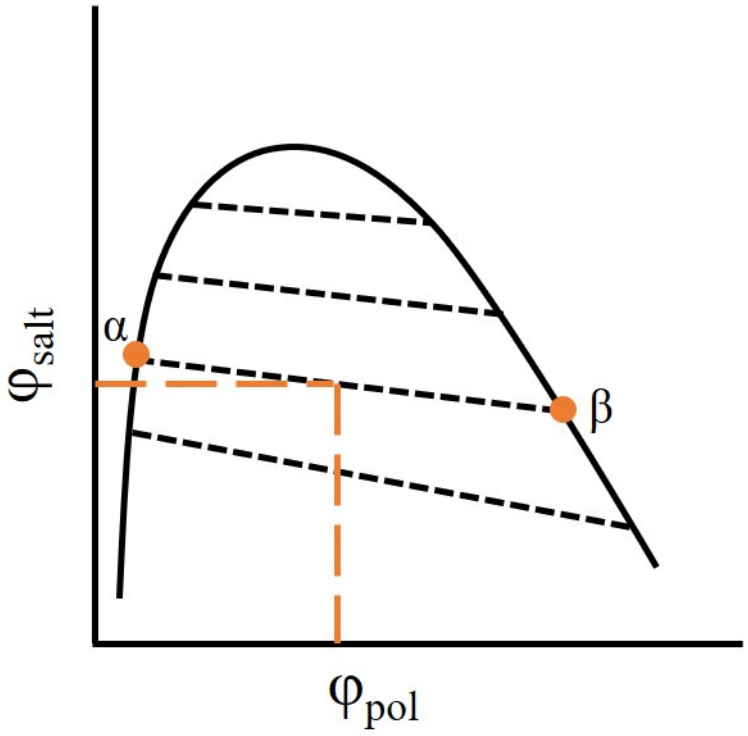

Figure 1: A schematic of a polyelectrolyte complex phase diagram. The axes are volume fraction of polymer, (ϕ_{pol}) and volume fraction of salt, (ϕ_{salt}). Samples prepared below the boundary separate into two phases, a polymer-poor phase, α, and polymer-rich phase, β. Tie-lines are represented by dashed lines between α and β. Above the boundary, the sample remains in a single phase.

1.1.2 Theoretical and Experimental Results of Modern Coacervate Phase Behavior

In order to develop a more sophisticated model for polyelectrolyte complex phase behavior, Li and coworkers used thermogravimetric analysis and molecular dynamic simulations to quantify phase behavior in polyelectrolyte complex systems and gain insight to molecular contributions. Interestingly, they found the tie-lines sloped downward contradicting the Voorn-Overbeek model. They concluded this was a result of excluded volume effects expelling salt counter ions from the coacervate phase, a contribution not included in the Voorn-Overbeek theory.[22]

Radhakrisna *et al.* used Motel Carlo simulations with varied charge spacing and hard-core excluded volume effects. Using recent Liquid State theory predictions and their Monte Carlo simulations, Radhakrisna *et al.* concluded that the success of the Voorn-Overbeek theory resides in the fortuitous cancellation of excluded volume and chain connectivity effects.[30,32] The Perry group tested these conclusions by synthesizing and studying sequence controlled polypeptides to determine the impact of precise placement of charged monomers on polyelectrolyte complex phase behavior. They found the behavior was dominated by the entropic release of the condensed counterion cloud and agreed well with the Monte Carlo simulations of phase behavior, which includes excluded volume and, more importantly, charge spacing specificity. Including these effects significantly improve the accuracy of modern theories of phase behavior.[2,33]

1.2 Viscoelasticity of Complex Coacervates

Complex coacervates have dynamic viscoelastic behavior that make them valuable tools in aqueous solutions. The viscoelastic behavior has been attributed to both the semi-dilute nature of the polymer solutions and the electrostatic interaction between the oppositely charged polymer chains.[34,35] Understanding the viscoelasticity can dramatically improve product design. Currently, the leading theory used to explain the viscoelastic behavior of

complex coacervates is the Sticky Rouse model, but it fails to account for both the volume fraction of polymer and the salt concentration without approximations.

1.2.1 Support of the Sticky Rouse Model

In 1998, Rubinstein and Semenov developed the Sticky Rouse model that explains viscoelastic behavior of associating polymer chains from the previously described Rouse model.[35–39] In its simplest form this model predicts that the terminal relaxation time of a material goes as:[34,40]

$$\tau_r = \tau_0 N^2$$

where τ_r is the terminal relaxation time of the sample, τ_0 is the relaxation of a single sticky site and N is the number of sticky sites. For complex coacervates, the Sticky Rouse model predicts that a single sticky point is the electrostatic association between charged sites on polymer chains.[27] More generally, the terminal relaxation time also depends on the volume fraction of polymer:

$$\tau_r = \tau_0 \phi^\beta N^2$$

In the volume fraction dependent terminal relaxation time, the volume fraction of polymer is denoted by ϕ and scales by some value of β, a term is often neglected in analysis of coacervate systems although the validity of this approximation has recently been called into question.

A number of experimental groups have attempted to test this model. Spruijt *et al.* discovered a time-salt superposition principle for coacervate relaxation behavior similar to the classic time-temperature superposition principle for polymer systems. The time-salt superposition principle assumes that all viscoelastic relaxation modes have the same salt dependence and that it is possible to collapse all salt concentration dependent moduli onto a single master curve if shifted by appropriate salt dependent shift factors.[41] Furthermore, Schlenoff *et al.* prepared polyelectrolyte complexes via salt doping, dissolution, and reprecipitation in order to determine the composition of the solid-like and liquid-like complex coacervates at equilibrium. They found the flow behavior correctly correlated to the salt concentration regardless of preparation method.[1] Using mixtures of stoichiometric and non-stoichiometric amounts of oppositely charged polymer chains, Spruijt and coworkers also performed a series of rheo-

logical measurements to probe molecular dynamics. They found the dynamics seemed to be well-predicted by the Sticky Rouse model. The mixtures of different chain lengths for polyanions and polycations were found to impact the dynamics differently: when changing the polycation chain length they observed larger relaxation behavior changes than when changing the polyanion. This suggests further research on chain length variations is needed.[3] Furthermore, these studies all ignored contributions from changes in the polymer volume fraction, which will prove important for the more sophisticated systems as discussed in the next section.

The Schlenoff group performed experiments on a nano-scanning electron microscope to evaluate the impact of rinsing or submerging polyelectrolyte complexes in water or organic solvents. They found distinctive pores in coacervates after they were submerged in water for just 24 hours.[42] Furthermore, they used small-angle neutron scattering to understand the impact of salt on the radius of gyration of poly(styrene sulfonate) independently in solution and in a polyelectrolyte complex in both the coacervate and supernatant phase. For the poly(styrene sulfonate) alone in solution, the radius of gyration decreased and the polymer coil shrank with increasing salt concentration. On the other hand, in the complex, the radius of gyration remained constant until the complex transitioned from a solid to a liquid coacervate, at which point they observed a decrease in coil size. They also observed an increase in porosity, similar to the results seen in their previous research on submerged polyelectolyte complexes.[43] Similarly, using a rheometer in a parallel plate configuration submerged in salt water or pure de-ionized water, the Colby group attempted to understand the viscoelastic response of swelling polyelectrolyte complexes. With these submerged systems, they found good agreement for low molecular weight polymer systems with the Sticky Rouse model, where terminal relaxation scales as a single relaxation multiplied by the number of sticky points squared.[44] They did not account for the pores discovered by the Schlenoff group, suggesting further research should be done to resolve these contradictory results. Although the Sticky Rouse model has had significant success describing the viscoelastic relaxation behavior of complex coacervates, difficulty disentangling the effects of polymer volume fraction and salt dependence has driven research to understand the limitations of this model.

1.2.2 Failings of the Sticky Rouse Model

In order to test the validity of the time-salt superposition for complex coacervates, Ali *et al.* performed small-amplitude oscillatory shear rheology measurements on coacervates at a wide range of temperatures and salt concentrations. They found that time-salt superposition is valid at high salt concentrations but begins to break-down as the coacervates approach the gel point and rubbery regime due to physical crosslinking dominating the relaxation dynamics. They were also unable to fit data without assuming that the polymer volume fraction contributions scales exponentially with β equal to 7/3.[45] The Perry group used rheological characterization of polyelectrolyte complexes to probe the solid-to-liquid transition with increasing salt concentration. Their results show it is impossible to perform a time-salt superposition across both solid and liquid coacervates and suggested solid-like behavior was a result of ionic cross-linking.[46] Furthermore, when using small angle X-ray scattering and rheological measurements, the Tirrell group compared arrangements of polymer chains on a molecular scale with bulk relaxation dynamics in both semidilute polymer solutions and polyelectolyte complex coacervates. They found similar scattering and rheological behavior but were not able to fit the shift factors and salt concentration curves without including the approximations for the polymer volume fraction.[47]

The assumptions made about the terminal relaxation time dependence on the polymer volume fraction and the difficulty in disentangling the volume fraction of polymer from the salt dependence has driven the research presented here. Using a specific sample preparation method in which we add salt to a pre-formed coacervate, we are able to disentangle these variables and probe the salt dependence, the polymer volume fraction, and the impact of cooperativity of charged sites.

2.0 Salt-Addition Experiment

In order to independently test the salt and polymer volume fraction dependence of complex coacervates, a series of complex coacervates were prepared and separated from their supernatant. A controlled amount of solid potassium bromide was added to these samples in varying amounts in order to change the salt concentration while holding the polymer volume fraction constant. These samples were then measured with thermogravimetric analysis to quantify their final compositions and small-amplitude oscillatory shear rheology measurements to analyze their characteristic relaxation times.

2.1 Introduction

As described in chapter 1, current literature suggests that complex coacervate viscoelastic behavior is dependent on both the salt concentration and the volume fraction of polymer. Up until now, no materials have been developed to experimentally separate the two variables. The difficulty lies in the current sample preparation methods, which change both the salt and polymer volume fraction in the coacervate, simultaneously. There has been substantial research into the impact of varying the salt concentration while making approximations about the polymer volume fraction.

In order to investigate this problem, a unique sample preparation method was developed, whereby a polyelectrolyte sample is prepared in bulk and the supernatant is removed. The coacervate phase is then separated into separate vials and solid potassium bromide is added to change the salt concentration while holding the volume fraction of polymer consistent. We verified the success of this method via thermogravimetric analysis and tested the viscoelastic properties of the resulting coacervates with small-amplitude oscillatory shear rheology.

2.2 Experimental Design

2.2.1 Materials

Poly(sodium 4-styrenesulfonate) (M_w = 200,000 g/mol) and poly(diallyldimethyl ammonium chloride) (M_w = 200,000-350,000) were purchased from Sigma Aldrich, purified via dialysis in Milli-Q water, and lyophilized prior to use. Removal of small-molecule impurities was verified with ^{1}H NMR in D_2O. The potassium bromide (KBr) was also purchased from Sigma Aldrich and used as received.

2.2.2 Preparation of Polyelectrolyte Complexes

Polyelectrolyte complexes were made from stock solutions of poly(styrene sulfonate) (PSS) and poly(diallyldimethyl ammonium chloride) (PDADMAC). After purification of polymers, stock solutions of PSS and PDADMAC were made at concentrations of 0.5 M charged monomer units. A KBr stock solution was made with a target concentration of 4 M. Samples were prepared by sequential addition of the required amounts of PSS stock solution, water, KBr stock solution, and PDADMAC stock solution to reach a target volume of 50 mL at the target salt concentration and 0.125 M concentration of each charged monomer. After each addition, the sample was vortexed for 1 minute at 2000 rpm. The samples were then centrifuged for 5 minutes at 4000 rpm, left to equilibrate for 24 hours, and centrifuged again for 20 minutes. The samples were left to equilibrate for a minimum of 5 days. After equilibration, the supernatant was removed and the coacervate phase was divided into 5 or 6 individual vials, each containing approximately 0.5-0.9 g of coacervate. Each sample was weighed and the amount of KBr necessary to reach the final target salt concentration was added. The coacervate/salt mixture was stirred manually for 1 minute and left to equilibrate for a minimum of 1 week before measurement.

2.2.3 Thermogravimetric Analysis

Thermogravimetric analysis (TGA) measurements were carried out on a Q5000 IR Thermogravimetric Analyzer (TA Instruments) using a measurement protocol adapted from Li *et al.*[22] Each sample was loaded onto a platinum pan and heated to 100°C at a rate of 20°C/min. The sample was then held at an isotherm at 110 °C for 60 minutes to remove all excess water in the sample. The temperature was then ramped up to 610°C at a rate of 10°C/min. At 610°C, the sample was held at a second isotherm for 90 minutes to remove as much residual organic material as possible. Finally, the temperature was ramped up to 680°C at 10°C/min to complete the measurement.

2.2.4 Rheological Measurements

Small-amplitude oscillatory shear measurements were performed on an Anton Paar MCR 301 stress-controlled rheometer, using a sand-blasted 25 mm parallel plate geometry. All measurements were performed at a gap height of 250 μm. The temperature was held at 20°C using peltier plates, and an evaporation blocker was used to minimize evaporation over the course of the measurement. Previous studies using a similar setup suggested that polyelectrolyte complexes begin to exhibit effects of evaporation after approximately 5 hours.[3] To avoid this problem, our measurement protocol was designed to complete the full series of measurements in 3 hours.

Three experiments were carried out on each sample. First an amplitude sweep was performed from 0.1% to 100% at a frequency of 10 rad/s to determine the linear regime. This was followed by a flow curve from 0.01 s^{-1} to 100 s^{-1} and finally a frequency sweep from 600 rad/s to 0.1 rad/s with an accompanying strain sweep from 1% to 100% in order to improve instrument response at low frequencies. This strain sweep method has been shown to improve instrument sensitivity near the low torque instrument limit.[48]

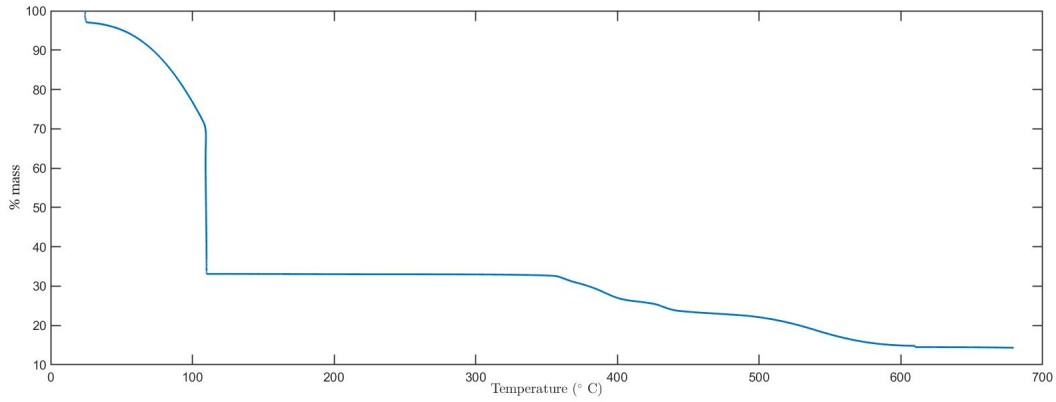

Figure 2: TGA trace of the 1.4 M KBr coacervate sample.

2.3 Results

2.3.1 TGA Results

TGA data was used to determine the composition of the initial coacervates and salt-added coacervates. Using the mass percentages taken from the TGA spectra, as seen in Fig. 2, we used bulk densities reported for the PSS/PDADMAC polymer system (1.13 g/mL), KBr (2.75 g/mL) and water (1.00 g/mL) to convert from mass to volume. The bulk density approximation has been used in previous work. Although there may be some non-ideal mixing in the samples, the bulk densities were assumed to be representative of the materials. The polymer, salt, and water volume fraction were calculated by dividing the calculated volumes of each component by the total calculated volume.

Using the TGA data, we constructed a phase diagram for this polymer system. As shown in Fig. 3, the coacervate has a significantly higher volume fraction of polymer than does the supernatant and there is a higher volume fraction of salt in the supernatant than the coacervate consistent with previous literature results. The composition of samples prepared by salt addition to each of these starting coacervates are shown in the same color. The TGA data shows that the polymer volume fraction is constant within the uncertainty of the

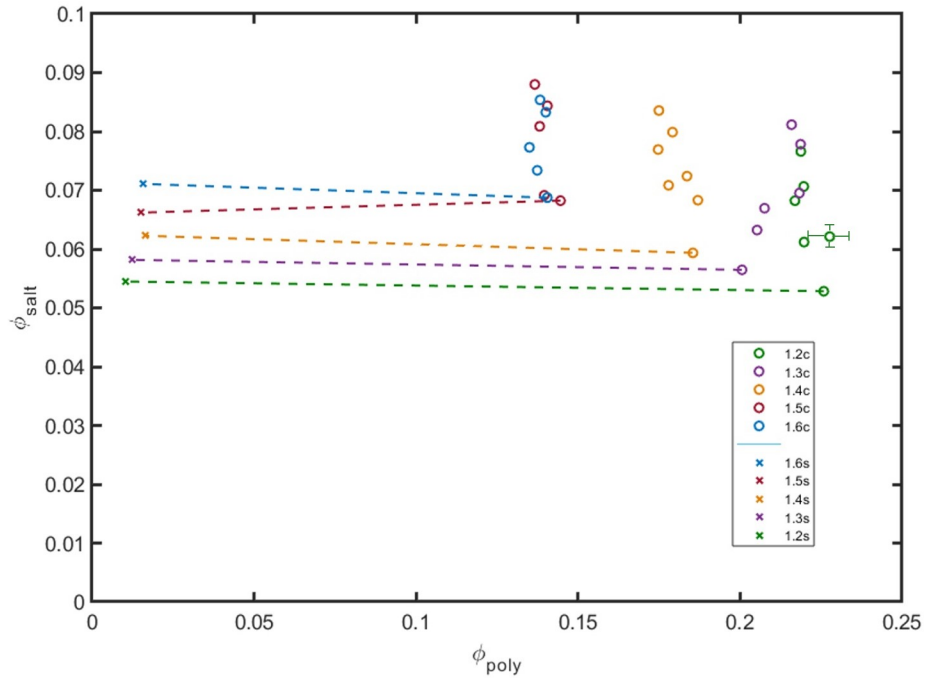

Figure 3: Phase diagram for the salt-addition experiment, using circles to represent the coacervate phase samples and crosses for the supernatant. Tie-lines are marked with dashed lines between the supernatant and the coacervate with no additional salt.

measurements within a single starting salt concentration series. This behavior allows us to independently compare the effect of both salt and polymer volume fraction on the rheological flow behavior to garner insight into the driving force behind polyelectrolyte complex flow behavior.

The highest polymer volume fraction occurs at the lowest initial salt concentration, matching previous literature studies of these materials. Interestingly, as the critical salt concentration is approached, at salt concentration of 1.5 M and 1.6 M, the polymer volume fraction is identical within the uncertainty of the measurement. This is possibly the result of approaching the critical salt concentration. These results allow us to analyze the salt and polymer concentration dependence on the rheological data, as describe below.

2.3.2 Rheological Data

Rheological measurements were used to determine how increasing the salt concentration in the coacervate phase impacts the viscoelastic behavior of coacervates when the polymer concentration is unchanged. As seen in Fig. 4, the lowest salt concentrations approach the gel point as seen by the deviation from the terminal regime flow behavior. For samples prepared at higher salt concentration, the moduli scaled as G' ω^2 and G" ω at low frequency indicating that they are in the terminal flow regime. These results match our predictions for complex coacervate rheology. With the addition of increasing amounts of salt, the moduli shift to lower magnitude and higher frequency, suggesting faster terminal relaxation times. Decreases in the terminal relaxation time have been suggested to be a result of either decreases in the polymer volume fraction or increases in the salt concentration. In the data shown in Fig. 4, we are able to completely attribute this change to the addition of salt, since there is no significant change in the polymer volume fraction in this series of samples. Furthermore, when exploring the impact of polymer volume fraction, while attempting to hold the salt concentration constant, seen in Fig. 5, there are still substantial changes in flow behavior as the polymer volume fraction varies. The decreasing polymer volume fraction, like the increasing salt concentration, causes a shift to higher frequencies and lower moduli. For deeper quantitative understanding between salt concentration and polymer volume fraction,

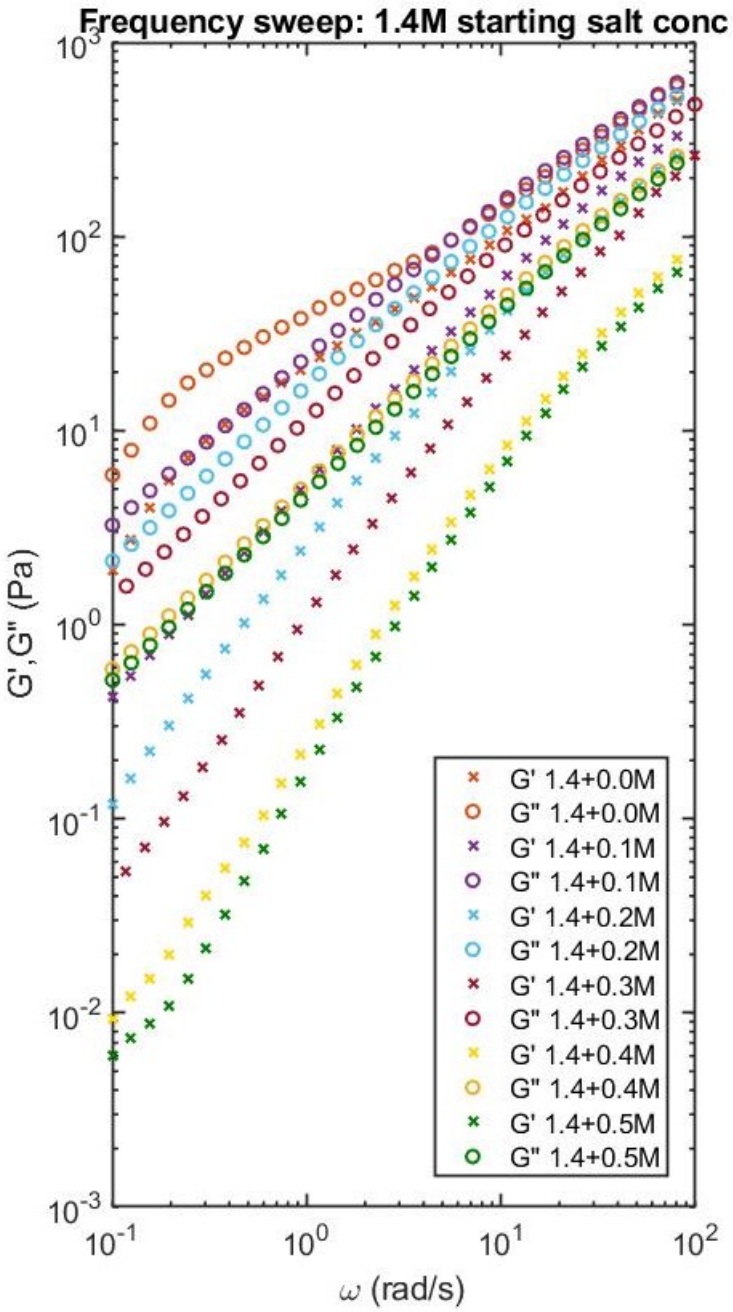

Figure 4: Raw rheology data for the series of samples with starting salt concentration of 1.4 M. As the salt concentration is increased the moduli shift to higher frequency.

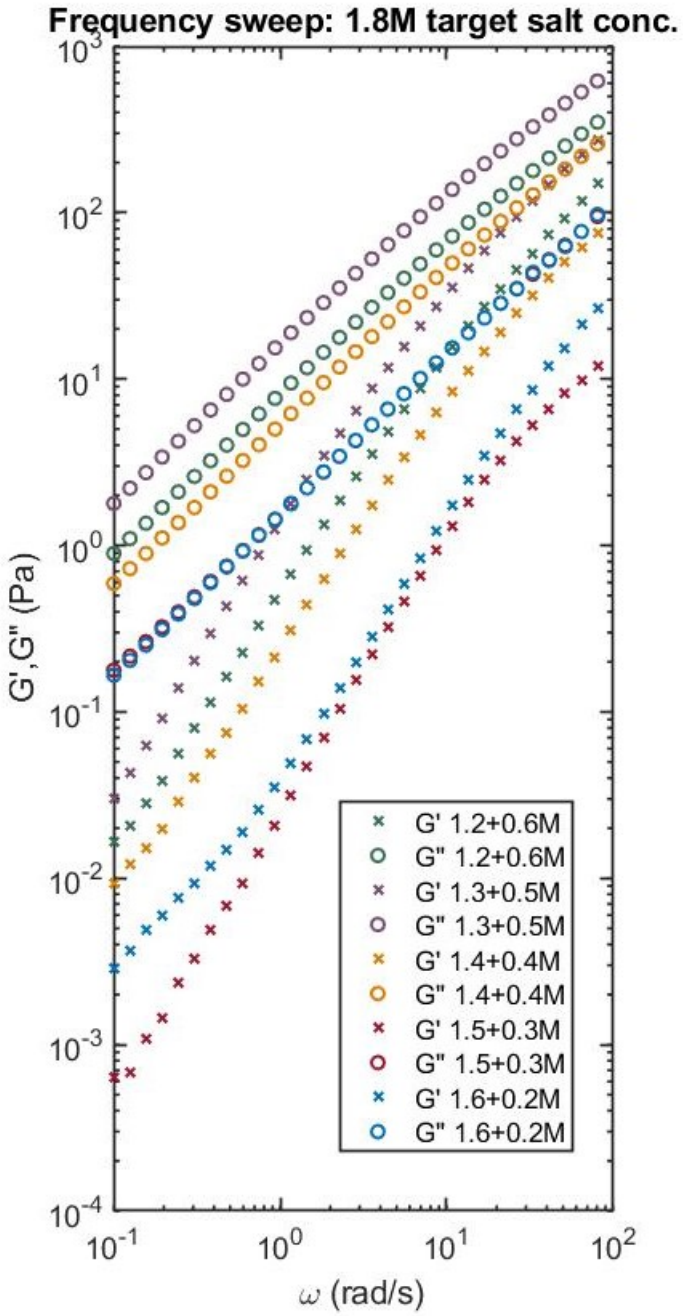

Figure 5: Raw rheology data for the series of samples with target salt concentration of 1.8 M. As the volume fraction of polymer increases the moduli shift to higher frequency.

these results will be explored in the next section by using a time-salt superposition to compare the horizontal shift factors to volume fraction of salt and polymer.

Using a time-salt superposition, we created a master curve for both the series with the same starting salt concentration and with the same target salt concentration. The horizontal shift factors give clear insight into how both the polymer volume fraction and the salt concentration impact the flow behavior of these viscoelastic materials. The Rubenstein group has posited that the terminal relaxation time for complex coacervates is given by the volume fraction dependent τ_r. Using this equation and our results, we are able to extract values of β by comparing our volume fraction of salt and polymer with our horizontal shift factors. The literature values of β generally are assumed to be between 1 and 2 depending on the approximations used. Rubenstein and Semenov suggested that the β value could go up to 6 in semi-dilute polymer solutions with associating sticky points.[34] As shown in Fig. 6, the value of β for different starting salt concentrations in this work varies from approximately 3 to 9, with higher β values for the samples with higher polymer volume fraction. When comparing all the absolute horizontal shift factors with the salt concentration, we found the overall β value to be -5.82 ± 0.54. The linear fit for this β value is a reasonable fit within the error of the measurement. These β values are significantly higher than the theoretical values or approximations used in previous work, suggesting our current understanding of complex coacervates is incomplete.

To analyze the salt dependence, we assume that the relaxation of a single electrostatic association goes as $\tau_0 \sim c_s^{\alpha}$, reflecting changes in the activation barrier for electrostatic association with salt concentration. When comparing samples with similar target salt concentration, we were able to calculate the value of α, representing the scaling associated with the salt concentration. Using a similar model to the time-salt superposition, we calculated shift factors of samples with decreasing polymer volume fraction. In doing so, we assume that the volume fraction of polymer impacts each mode of relaxation equally. Although there are no direct studies of shifting polymer volume fraction while maintaining salt concentration and temperature, this model suggests that the time-polymer volume fraction superposition is successful for this system. We found values of 1.79 ± 0.24 for α as seen in Fig. 8. More research is needed to fully understand the activation energy dependence on

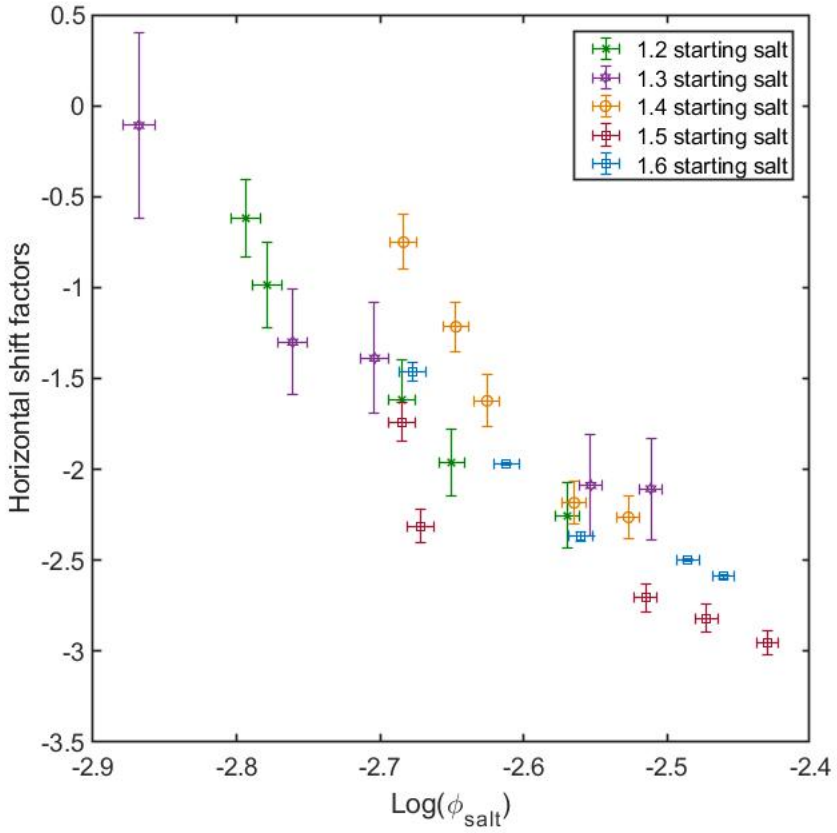

Figure 6: On a logarithmic scale, the absolute horizontal shift factors and volume fraction of salt at the different starting salt concentrations collapse onto a single line. The slope of this line giving the value of the scaling exponent β.

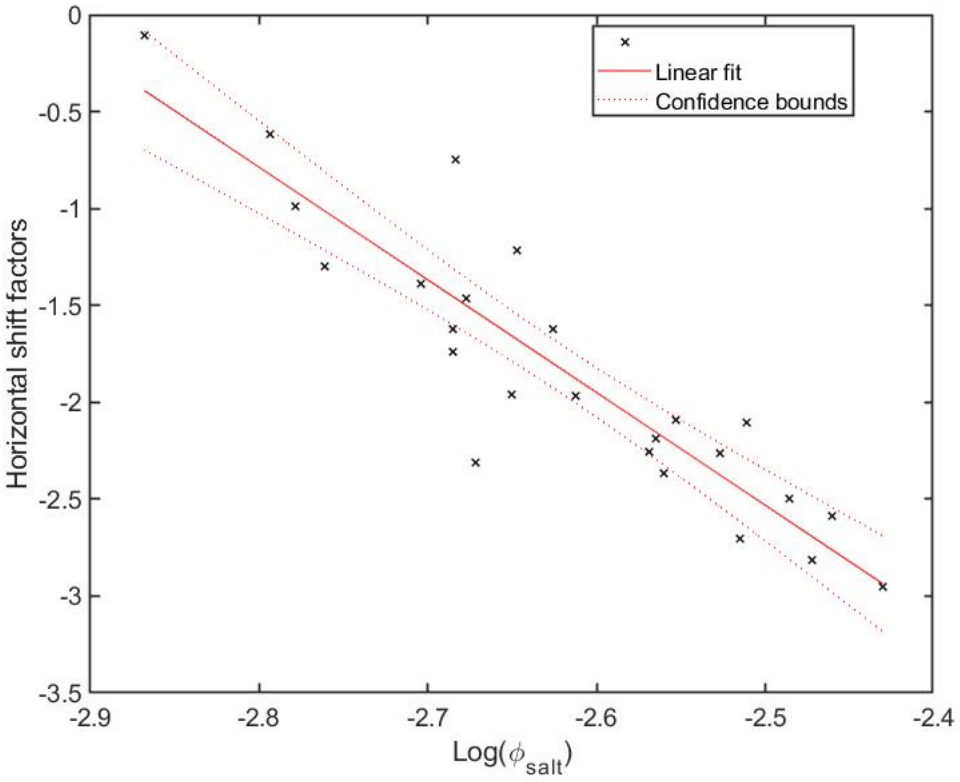

Figure 7: A linear fit, with 95% confidence, was used to determine the value of β from the horizontal shift factors and volume fraction of salt, as seen in Fig. 6.

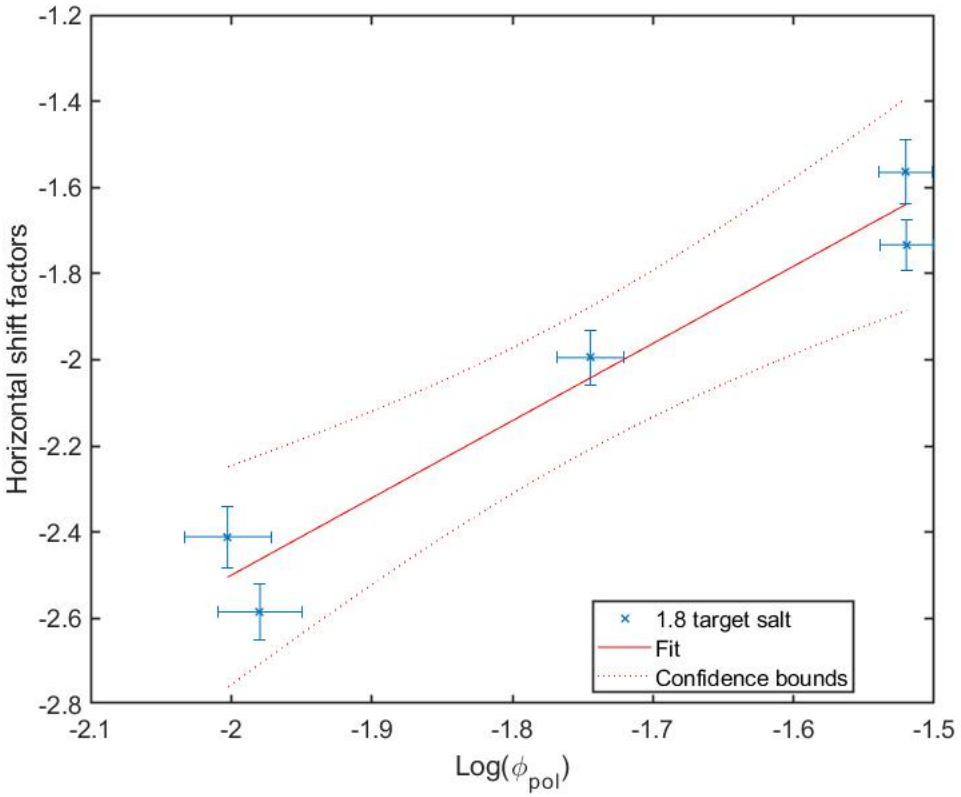

Figure 8: Absolute horizontal shift factors and the polymer volume fraction to determine the value of α and the 95% confidence of the fit.

salt concentration.

2.4 Discussion

The shift to higher frequencies and lower moduli shown in Fig. 4 for the series of samples with the same starting salt concentration can be attributed to the increasing amount of added salt. The current polyelectrolyte complex theory suggests that with increases in salt concentration, the salt ions are able to disrupt the sticky sites or ionic linkages acting as reversible cross-links between polymer chains, speeding up the terminal relaxation time.[27] Although this may not be a complete picture of the complexities of the dynamics of these materials, there is significant dependence of the viscoelastic properties on the salt concentration. Conversely, the rheological shifts seen in Fig. 5 for a series of samples with the same target salt concentration can be attributed to the changes in polymer volume fraction. This suggests that the decrease in polymer volume fraction also causes faster terminal relaxation of the chains. This change has been attributed to the diffusion of polymers in a semi-dilute solution. This behavior is theorized to be result of polymer diffusion: a lower volume fraction allows for faster polymer chain relaxation irrespective of salt concentration.[26] Despite the difficulty disentangling these variables, our results suggest that the dependence on salt concentration and polymer volume fraction can be independently tested. Although this may not be a complete picture of the complexities of the dynamics of these materials, these results have shown that the flow behavior is not exclusively dominated by the salt dependence or the volume fraction of polymer.

This research provides context for a new method of studying complex coacervates. The polymer volume fraction scaling exponent β is significantly higher than previous approximations have assumed. This suggests that the polymer volume fraction plays a substantially larger role in the relaxation dynamics of these complex coacervates. Furthermore, the ability to disentangle the polymer and salt volume fraction increase our understanding of the driving forces behind the viscoelasic behavior of coacervates. Moving forward, this research provides a unique approach to developing tunable properties of the polyelectrolyte complexes. With

the ability to independently vary the polymer or salt volume fraction, the versatility of these materials will increase. This will provide further insight into the our understanding of these materials as well as our methodology for product design.

2.5 Acknowledgements

I would like to thank Yan Wang and Leanne Gilbertson in the Swanson School of Engineering for their help with the TGA measurements and access to the TGA. I would also like to thank Anqi Wang and Jung-Kun Lee in the Swanson School of Engineering for access to their MCR-301 for the measurements done here.

3.0 Charge Density Experiment

A series of copolymers were synthesized with decreasing charge density and measured with small-amplitude oscillatory shear rheology measurements. These measurements provided insight into the impact of molecular charge spacing on the bulk rheological flow behavior of complex coacervates. The dispersity and number of charged sites on these polymer chains were carefully controlled in order to probe cooperativity between charged sites. The preliminary data indicate that the interaction between multiple charged sites may be more complex than the Sticky Rouse model currently predicts. However, experimental inconsistencies prevented a full data set from being collected and more work will be needed before conclusions can be determined.

3.1 Introduction

The Sticky Rouse model makes a critical assumption that the terminal relaxation time depends on the relaxation of a single sticky point and number of sticky sites squared, as seen in simple terminal relaxation equation. In this model, the τ_0 term scales exponentially as the activation energy of dissociation of a single electrostatic interaction, which depends on the salt concentration. This model fails to take into account separation between sticky points or cooperativity of charged sites and assumes that the activation energy of a single sticky point is consistent regardless of the surrounding environment. The Perry and Sing groups have done a substantial amount of theoretical work on this topic and some experimental phase behavior research.[6,31,33] Despite this research, the ability to probe the activation energy of these sticky sites has yet to be developed in complex coacervates.

Here, we address this problem by investigating the viscoelasticity of coacervates formed from poly(acrylic acid) and poly(dimethyl amino ethyl methacrylate-*co*-diethylene glycol methyl ether methacrylate). The polymers were designed such that they have similar number of charged sites, targeting 200 charged monomer unit per chain. For the copolymers,

the number of dimethyl amino ethyl methacrylate monomers was held consistent while the molecular weight was increased, thus decreasing the charge density. This molecular change should give substantial insight into the cooperativity of charge sites and resulting impact of separating charged monomers on the bulk material behavior.

3.2 Experimental Design

3.2.1 Polymer synthesis

The poly(acrylic acid) was synthesized by atom transfer radical polymerization and the poly(dimethyl amino ethyl methacrylate-*co*-diethylene glycol methyl ether methacrylate) was synthesized by reversible addition-fragmentation chain-transfer polymerization, as described below.

3.2.1.1 Materials All materials were purchased from Sigma Aldrich. For the poly(acrylic acid) synthesis, ethyl-2-bromopropionate (EBrP), N,N,N',N',N"-pentamethyldiethylenetriamine (PMDETA),trifluoroacetic acid, and the solvents, anisole, dichloromethane, N,N-dimethylformamide and ethanol, were used as received. *Tert*-butyl acrylate was filtered through activated neutral alumina immediately before use. For the synthesis of poly(dimethyl amino ethyl methacrylate-*co*-diethylene glycol methyl ether methacrylate), dimethyl amino ethyl methacrylate (DMAEMA) and diethylene glycol methyl ether methacrylate (DEGMA), were filtered through activated neutral alumina immediately before use. Azobisisobutyronitrile (AIBN) recrystallized from methanol. N-ethyl piperidine hypophosphite, 4-cyano-4-[(dodecylsulfanylthiocarbonyl)sulfanyl]pentanoic acid, toluene and methanol were used as received.

3.2.1.2 Synthesis of Poly(acrylic acid) Poly(acrylic acid) (PAA) was synthesized by atom transfer radical polymerization of poly(*tert*-butyl acrylate) (PtBuA), followed by cleavage of the *tert*-butyl side-chain to produce PAA.[49] In a typical polymerization target-

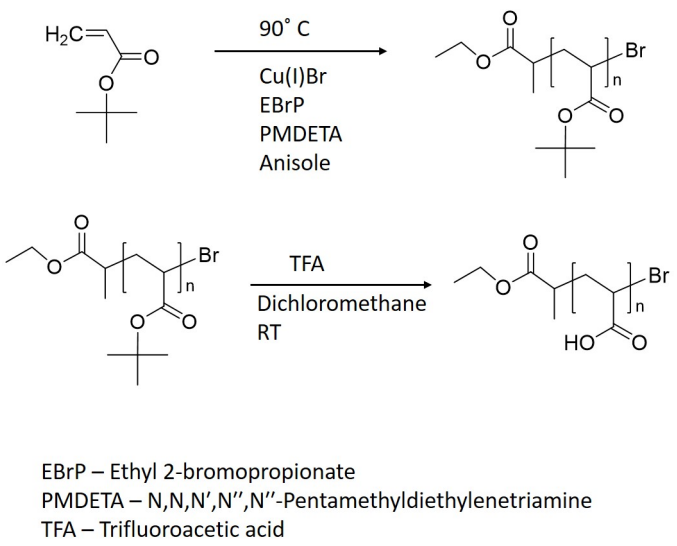

Figure 9: Reaction scheme: synthesis of poly(acrylic acid).

ing PtBuA with a molecular weight of 27 kg/mol, a Schlenk flask containing 0.297 g copper(I)bromide was sealed and placed in liquid nitrogen. While the flask was submerged in liquid nitrogen, a mixture of 106.5 g *tert*-butyl acrylate, 0.270 mL EBrP, 0.428 mL PMDETA, and 24 mL anisole was injected into the flask. Three freeze-pump-thaw cycles were performed to degas the mixture. The flask was then filled with argon and sealed and the reaction was performed at 90 °C for approximately 6 hours.

Aliquots of the reaction mixture were withdrawn at regular intervals, and the monomer conversion was monitored by ^{1}H nuclear magnetic resonance (NMR) in deuterated chloroform. When the conversion reached 50%, the reaction was quenched by removing the reaction flask from the heat and placing it in an ice bath. The mixture was then precipitated into 3 L of a 75% ethanol/25% water mixture. The precipitated PtBuA was redissolved in tetrahydrofuran (THF) and filtered through activated neutral alumina to remove the remaining copper. The mixture was then precipitated a second time and the recovered PtBuA was dried overnight under vacuum. The molecular weight and dispersity were determined by size exclusion chromatography (SEC) on an EcoSEC Elite GPC System (Tosoh Bioscience)

equipped with a multi-angle light scattering detector (Wyatt Heros II). The SEC measurements were performed at 40 °C in THF with a dn/dc value of 0.512.

The *tert*-butyl side chains were then cleaved to form PAA. Approximately 50% of the dried PtBuA (25 g, 1 eq. tBu) was dissolved in 125 mL dichloromethane. Trifluoroacetic acid (50 mL, 3.25 eq.) was then added to the mixture and the flask was sealed.[50] The mixture was stirred at room temperature for two days. Over the course of the reaction, the resulting PAA precipitated to form a white solid. The supernatant was then removed under reduced pressure and the solid was redissolved in a N,N-dimethylformamide and ethanol mixture. This mixture was sequentially dialyzed against pure ethanol, followed by a 50% ethanol/50%water mixture, and finally pure water. The water was finally removed by lyophilization. The purity and remaining *tert*-butyl content of the dried polymer were determined by ^{1}H NMR formation of PAA was confirmed by the loss of the large singlet at approximately 1.5 ppm corresponding to the t-butyl group, as shown in Fig. 18.

For simplicity in tables and figures poly(acrylic acid) will be represented by A.

3.2.1.3 Synthesis of Poly(dimethyl amino ethyl methacrylate-*co*-diethylene glycol methyl ether methacrylate) Poly(dimethyl amino ethyl methacrylate-*co*-diethylene glycol methyl ether methacrylate) (poly(DMAEMA-*co*-DEGMA)) was synthesized by reversible addition-fragmentation chain transfer (RAFT) polymerization. Each polymer had a targeted 200 DMAEMA monomer units per chain with increasing amounts of DEGMA comonomer.[51] This increase in DEGMA content decreases the charge density and increases the polymer molecular weight. The targeted ratios for DMAEMA to DEGMA monomers

Table 1: Poly(acrylic acid) used in preliminary experiments

Polymer	M_n (NMR, kg/mol)	M_n (SEC, kg/mol)	Đ	Monomer Ratio (%)
A	15	15	1.09	N/A

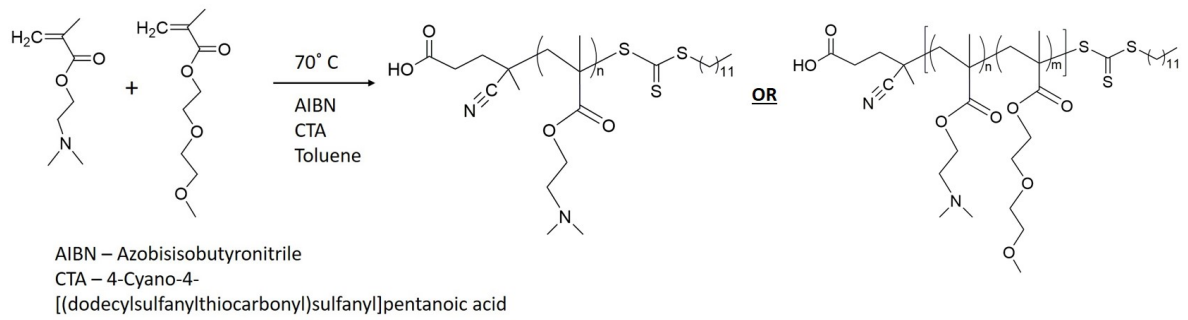

Figure 10: Reaction scheme: synthesis of poly(DMAEMA-*co*-DEGMA).

were 5:1, 3:1, and 2:1. In each synthesis the concentrations of DMAEMA, the chain transfer agent, and AIBN were held constant while the concentrations of DEGMA and toluene were changed to target the desired monomer ratios. In a typical polymerization (here the 5:1 copolymer), 29.2 g of DMAEMA monomer, 7.0 g of DEGMA, 272 mg of the chain transfer agent, 11.2 mg AIBN and 50 g of toluene were combined in a Schlenk flask. The flask was sealed and three freeze-pump-thaw cycles were performed to degas the mixture. The flask was then filled with argon and the mixture was polymerized for approximately 18 hours at 70 °C. Aliquots of the reaction mixture were withdrawn at regular intervals during the last 6 hours of the reaction to monitor monomer conversion by ^{1}H NMR in deuterated chloroform. When the reaction reach 73% conversion, the reaction was quenched by removing the flask from the heat and placing it in an ice bath. The mixture was precipitated into 3 L of cold hexanes, redissolved in toluene and precipitated a second time. The mixture was then dissolved in benzene and freeze-dried overnight under vacuum. SEC was used to determine the molecular weight and dispersity of the polymer sample. The measurement was performed in tetrahydrofuran with 1% triethylamine at 40 °C with a dn/dc value of 0.084 for poly(DMAEMA).

The trithiocarbonate end-group of the polymers was removed by a UV-light initiated reaction.[52] Each gram of polymer was dissolved in 6.5 g of toluene and 2.4 g of methanol with an excess of N-ethylpiperidine hypophosphite (48.8 mg, 3 eq.). The reaction flask was sealed and flushed with argon and the mixture was placed over a UV-light source (approx.

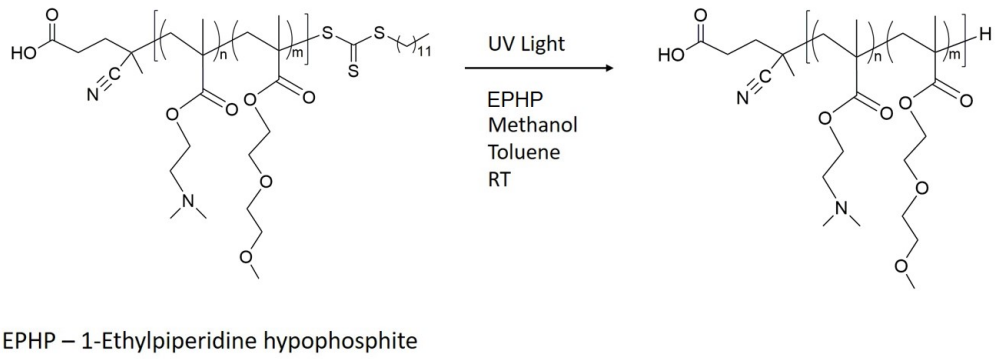

Figure 11: Reaction scheme: removal of trithiocarbonate end-group.

36 W at 365 nm) for 48 hours at room temperature with stirring. Success of the end-group removal was analyzed with UV-Vis Spectroscopy and the molecular weight and dispersity were measured again to verify no chain-chain termination occurred during end-group removal.

For simplicity in tables and figures, polymers will be described such that D represents DMAEMA monomers while G represents DEGMA monomers, for example DG (5:1) is poly(DMAEMA-*co*-DEGMA) at a 5:1 DMAEMA monomer to DEGMA monomer ratio.

Table 2: Poly(DMAEMA-*co*-DEGMA) used in preliminary experiments

Polymer	M_n (NMR, kg/mol)	M_n (SEC, kg/mol)	Đ	Monomer Ratio (%)
D	30	36	1.04	N/A
DG (5:1)	38	44	1.07	82.7
DG (3:1)	46	49	1.09	74.1
DG (2:1)	50	55	1.12	66.0

3.2.2 Preparation of Polyelectrolyte Complexes

Polyelectrolyte complexes were made from 0.5 M concentration of charged monomer stock solutions of PAA and poly(DMAEMA-*co*-DEGMA), and a 3 M stock solution of potassium chloride (KCl). The stock solutions were pH-adjusted to 6.5 ± 0.2 by adding concentrated hydrochloric acid (HCl) (Sigma Aldrich) or 50% wt. sodium hydroxide (NaOH) in MilliQ water. The samples were prepared by adding PAA, then water, KBr and poly(DMAEMA-*co*-DEGMA) to target a polymer concentration of 0.2 M. After each addition, the samples were vortexed for 1 minute at 2000 rpm. The samples were left to sit for 2 days and then centrifuged for 30 minutes and left to equilibrate for a minimum of 2 additional days.

3.2.3 Rheological Measurements

Small-amplitude oscillatory shear measurements were performed on an Anton Paar MCR-302 stress-controlled rheometer, using a 40mm cone and plate geometry with a cone angle of 0.3°. The measurements were performed at 25°C with an evaporation blocker to prevent significant evaporation effects on the samples. All experiments were performed in under 3 hours to avoid any substantial evaporation of the aqueous solvent. Two experiments were performed on each sample, an amplitude sweep from 0.1% to 100% at a frequency of 10 rad/s and a frequency sweep from 600 rad/s and 0.01 rad/s at a strain of 1%.

3.3 Results and Conclusions

Rheological measurements were used to determine the viscoelastic flow behavior of the polyelectrolyte complexes with decreasing polycation charge density. The Sticky Rouse model suggests that regardless of spacing between charge sites, the terminal relaxation depends only on the number of sites and the relaxation of a single sticky site. This should result in identical viscoelastic responses despite the decreasing charge density. This result was not supported by the preliminary rheological results gathered from this weak polyelectrolyte system. With decreasing charge density, the moduli shifted down and to higher frequencies, as

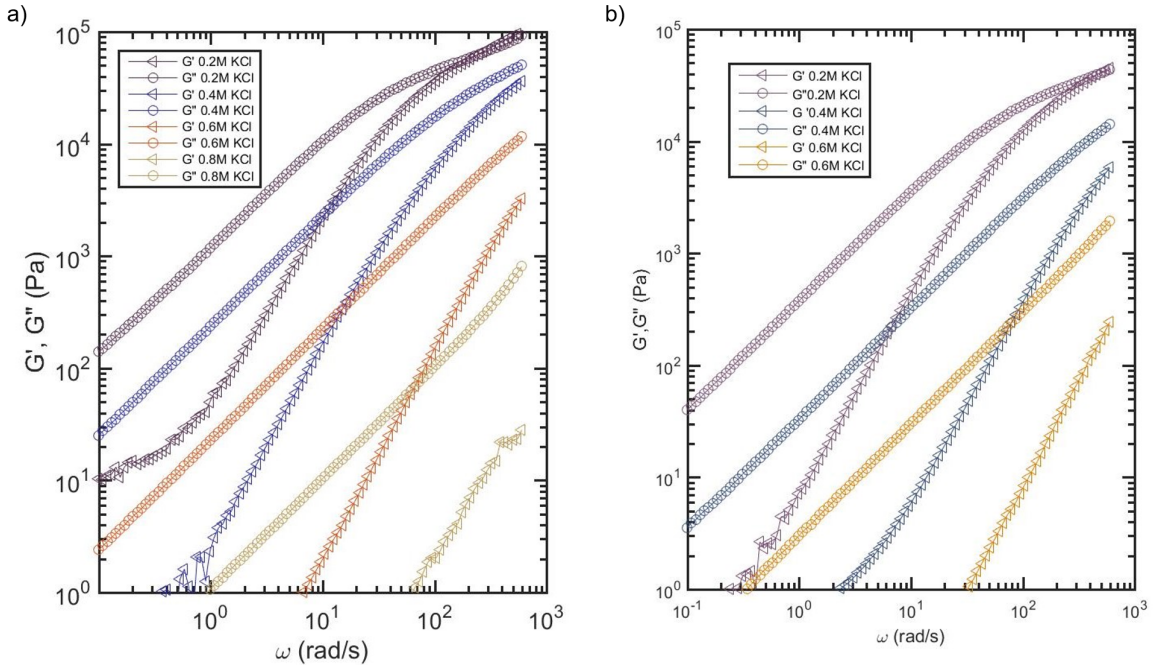

Figure 12: Raw rheological results of (a) D and A and (b) DG(5:1) and A.

seen in Fig. 12. Using a time-salt superposition, we were able to shift the moduli into a master curve and extract preliminary horizontal shift factors. The decrease in charge density causes the horizontal shift factors to decrease suggesting that the Sticky Rouse model is more complex than previously thought. The decrease in charge density suggest that the cooperativity between charges impacts the activation energy and relaxation of a single sticky site and thus changes the terminal relaxation. As shown in Fig. 14, as the charge density decreases, the horizontal shift factors decrease at different rates, suggesting a dependence on the cooperativity of electrostatic interactions. Although these preliminary results suggest that there is some charge density dependence, interpretation of this data is complicated by changes in volume fraction of polymer with decreasing charge density. The total coacervate volume increased when the fraction of DEGMA monomers increased. The total volume of coacervate, as estimated from pictures seen in Fig. 15, was used to calculated the polymer volume fraction with the assumption that 100% of the polymers chains are contained within

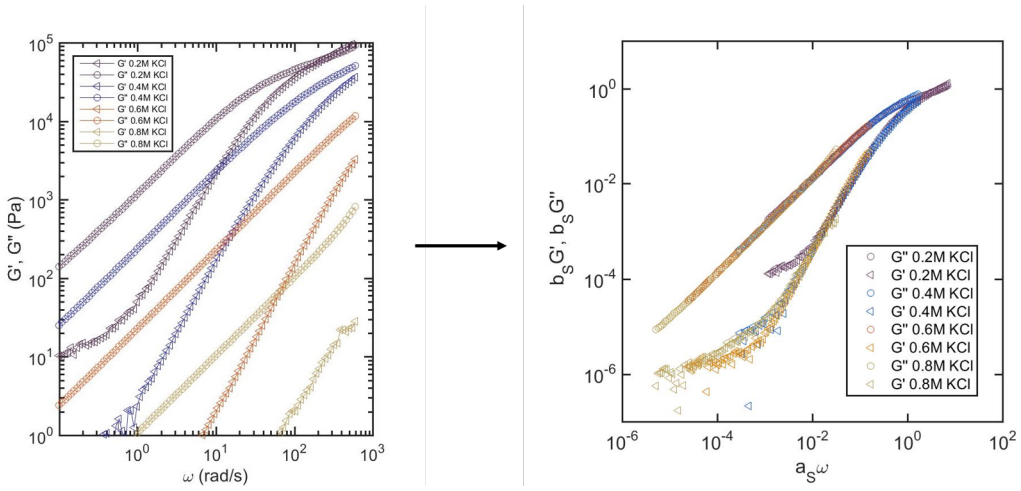

Figure 13: Using horizontal and vertical shift factors, the individual rheological traces were overlayed to form a master curve for the D and A polymer.

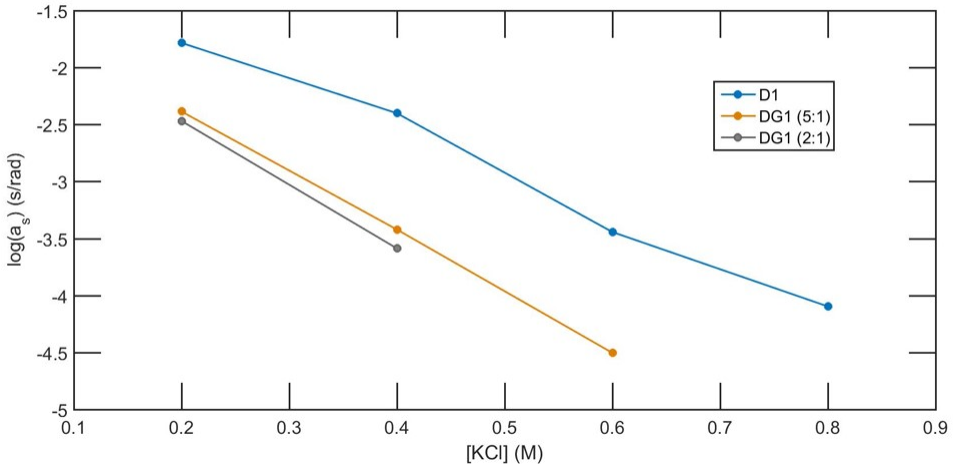

Figure 14: Plotting the salt concentration versus the horizontal shift factors for the different charge density systems.

the coacervate phase. This is a reasonable assumption, as shown in the previous chapter, because the amount of polymer present in the supernatant phase is small. This shift in the volume fraction of polymer makes it difficult to attribute the changes in relaxation time to only the cooperativity of charged sites. This suggests that, in order to further disentangle individual activation energy from the volume fraction of polymer, a series of salt-addition experiments on the decreasing charge density polymer series should be performed.

Unfortunately, when attempting to repeat these measurements, there was difficulty with sample reproducibility. Due to the difficult nature of weak polyelectrolyte systems, despite measures set in place to limit variability, samples prepared in identical manners would exhibit vastly different phase behavior and viscoelastic properties. Fig. 16 presents a series of samples produced from the same polymer with identical solution and preparation method. A series of experiments to carefully control and test the effects of equilibration time, pH, temperature and stoichiometry of polyelectrolyte complexes were performed. Despite this research and control measures, there was still significant variability between different samples. Significantly more research needs to be done to improve the weak polyelectolyte sample preparation methods in order to improve reproducibility.

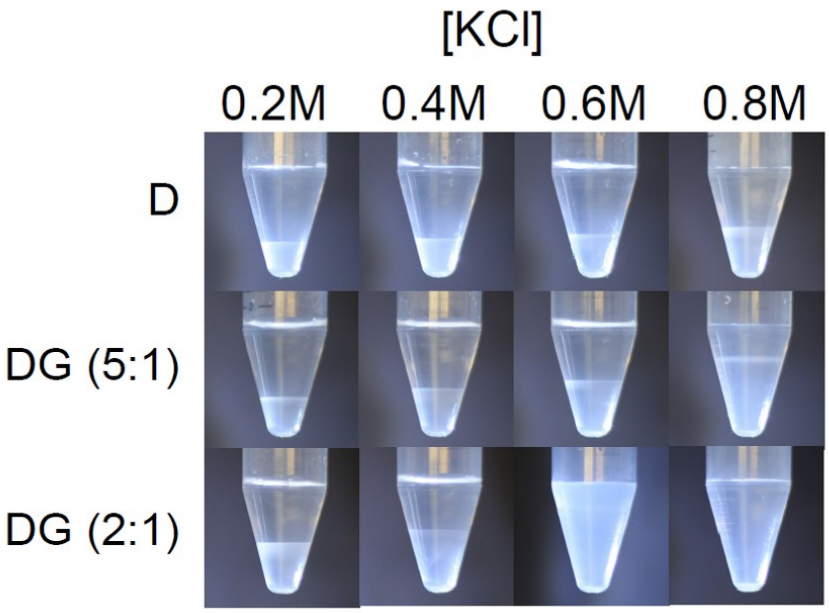

Figure 15: Changes in charge density at different salt concentration show an overall coacervate volume change suggesting a polymer volume fraction change.

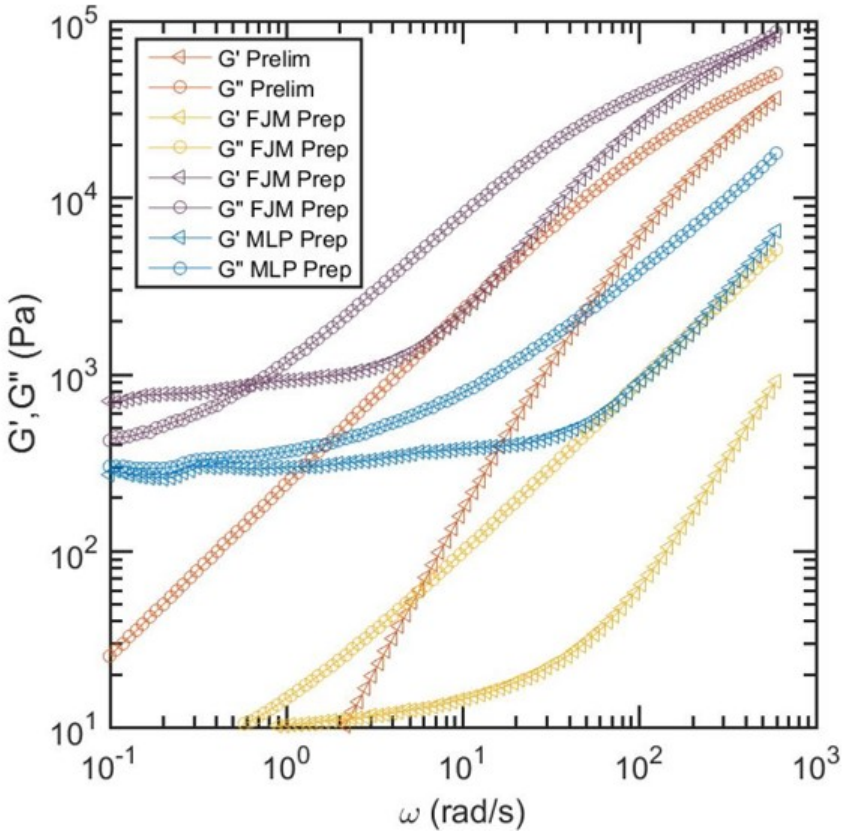

Figure 16: A series of polymers prepared with as little variability as possible. There is a dramatic change in viscoelastic behavior, suggesting reproducibility problems in weak polyelectrolyte systems.

Appendix

Supporting Information for: Charge Density Experiment

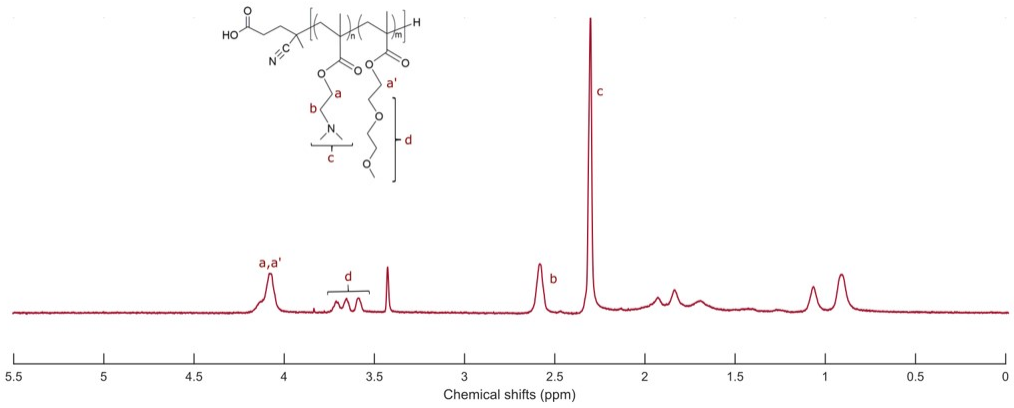

Figure 17: NMR data for the 5:1 poly(DMAEMA-*co*-DEGMA) after end group removal.

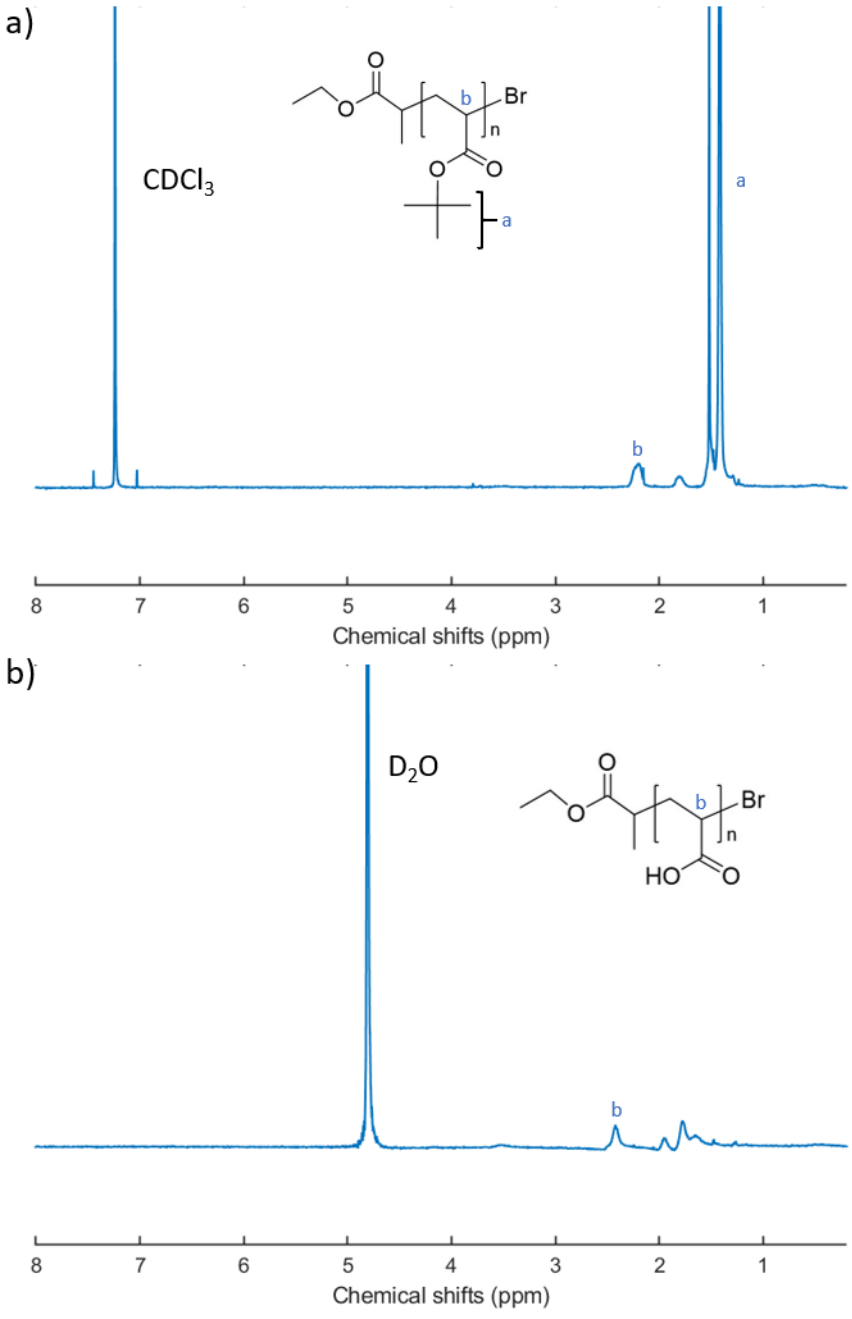

Figure 18: NMR data showing the removal of the *tert*-butyl group.

Bibliography

[1] Wang, Q.; Schlenoff, J. B. The Polyelectrolyte Complex/Coacervate Continuum. *Macromolecules* **2014**, *47*, 3108–3116.

[2] Chang, L.-W.; Lytle, T. K.; Radhakrishna, M.; Madinya, J. J.; Vélez, J.; Sing, C. E.; Perry, S. L. Sequence and entropy-based control of complex coacervates. *Nature Communications* **2017**, *8*.

[3] Spruijt, E.; Stuart, M. A. C.; van der Gucht, J. Linear Viscoelasticity of Polyelectrolyte Complex Coacervates. *Macromolecules* **2013**, *46*, 1633–1641.

[4] Gucht, J. v. d.; Spruijt, E.; Lemmers, M.; Cohen Stuart, M. A. Polyelectrolyte complexes: Bulk phases and colloidal systems. *Journal of Colloid and Interface Science* **2011**, *361*, 407–422.

[5] Sadman, K.; Wang, Q.; Chen, Y.; Keshavarz, B.; Jiang, Z.; Shull, K. R. Influence of Hydrophobicity on Polyelectrolyte Complexation. *Macromolecules* **2017**, *50*, 9417–9426.

[6] Perry, S.; Li, Y.; Priftis, D.; Leon, L.; Tirrell, M. The Effect of Salt on the Complex Coacervation of Vinyl Polyelectrolytes. *Polymers* **2014**, *6*, 1756–1772.

[7] Tekaat, M.; Bütergerds, D.; Schönhoff, M.; Fery, A.; Cramer, C. Scaling properties of the shear modulus of polyelectrolyte complex coacervates: a time-pH superposition principle. *Physical Chemistry Chemical Physics* **2015**, *17*, 22552–22556.

[8] Lou, J.; Friedowitz, S.; Qin, J.; Xia, Y. Tunable Coacervation of Well-Defined Homologous Polyanions and Polycations by Local Polarity. *ACS Central Science* **2019**, *5*, 549–557.

[9] Yang, M.; Shi, J.; Schlenoff, J. B. Control of Dynamics in Polyelectrolyte Complexes by Temperature and Salt. *Macromolecules* **2019**, *52*, 1930–1941.

[10] Waite, J. H.; Andersen, N. H.; Jewhurst, S.; Sun, C. Mussel Adhesion: Finding the Tricks Worth Mimicking. *The Journal of Adhesion* **2005**, *81*, 297–317.

[11] Lim, S.; Choi, Y. S.; Kang, D. G.; Song, Y. H.; Cha, H. J. The adhesive properties of coacervated recombinant hybrid mussel adhesive proteins. *Biomaterials* **2010**, *31*, 3715–3722.

[12] Winslow, B. D.; Shao, H.; Stewart, R. J.; Tresco, P. A. Biocompatibility of adhesive complex coacervates modeled after the sandcastle glue of Phragmatopoma californica for craniofacial reconstruction. *Biomaterials* **2010**, *31*, 9373–9381.

[13] Shao, H.; Bachus, K. N.; Stewart, R. J. A Water-Borne Adhesive Modeled after the Sandcastle Glue ofP. californica. *Macromolecular Bioscience* **2009**, *9*, 464–471.

[14] Kaur, S.; Weerasekare, G. M.; Stewart, R. J. Multiphase Adhesive Coacervates Inspired by the Sandcastle Worm. *ACS Applied Materials & Interfaces* **2011**, *3*, 941–944.

[15] Shao, H.; Stewart, R. J. Biomimetic Underwater Adhesives with Environmentally Triggered Setting Mechanisms. *Advanced Materials* **2010**, *22*, 729–733.

[16] Stewart, R. J.; Wang, C. S.; Shao, H. Complex coacervates as a foundation for synthetic underwater adhesives. *Advances in Colloid and Interface Science* **2011**, *167*, 85–93.

[17] Zhao, Q.; Lee, D. W.; Ahn, B. K.; Seo, S.; Kaufman, Y.; Israelachvili, J. N.; Waite, J. H. Underwater contact adhesion and microarchitecture in polyelectrolyte complexes actuated by solvent exchange. *Nature Materials* **2016**, *15*, 407–412.

[18] Wang, D.; Gong, X.; Heeger, P. S.; Rininsland, F.; Bazan, G. C.; Heeger, A. J. Biosensors from conjugated polyelectrolyte complexes. *Proceedings of the National Academy of Sciences* **2001**, *99*, 49–53.

[19] Black, K. A.; Priftis, D.; Perry, S. L.; Yip, J.; Byun, W. Y.; Tirrell, M. Protein Encapsulation via Polypeptide Complex Coacervation. *ACS Macro Letters* **2014**, *3*, 1088–1091.

[20] Xing, F.; Cheng, G.; Yi, K.; Ma, L. Nanoencapsulation of capsaicin by complex coacervation of gelatin, acacia, and tannins. *Journal of Applied Polymer Science* **2005**, *96*, 2225–2229.

[21] Devi, N.; Sarmah, M.; Khatun, B.; Maji, T. K. Encapsulation of active ingredients in polysaccharide–protein complex coacervates. *Advances in Colloid and Interface Science* **2017**, *239*, 136–145.

[22] Li, L.; Srivastava, S.; Andreev, M.; Marciel, A. B.; de Pablo, J. J.; Tirrell, M. V. Phase Behavior and Salt Partitioning in Polyelectrolyte Complex Coacervates. *Macromolecules* **2018**, *51*, 2988–2995.

[23] Overbeek, J. T. G.; Voorn, M. J. Phase separation in polyelectrolyte solutions. Theory of complex coacervation. *Journal of Cellular and Comparative Physiology* **1957**, *49*, 7–26.

[24] Flory, P. J. Thermodynamics of High Polymer Solutions. *The Journal of Chemical Physics* **1942**, *10*, 51–61.

[25] Huggins, M. L. Solutions of Long Chain Compounds. *The Journal of Chemical Physics* **1941**, *9*, 440–440.

[26] Hiemenz, P. C.; Lodge, T. P. *Polymer Chemistry*; CRC Press, 2007.

[27] Spruijt, E.; Westphal, A. H.; Borst, J. W.; Stuart, M. A. C.; van der Gucht, J. Binodal Compositions of Polyelectrolyte Complexes. *Macromolecules* **2010**, *43*, 6476–6484.

[28] Priftis, D.; Xia, X.; Margossian, K. O.; Perry, S. L.; Leon, L.; Qin, J.; de Pablo, J. J.; Tirrell, M. Ternary, Tunable Polyelectrolyte Complex Fluids Driven by Complex Coacervation. *Macromolecules* **2014**, *47*, 3076–3085.

[29] Jha, P.; Desai, P.; Li, J.; Larson, R. pH and Salt Effects on the Associative Phase Separation of Oppositely Charged Polyelectrolytes. *Polymers* **2014**, *6*, 1414–1436.

[30] Radhakrishna, M.; Basu, K.; Liu, Y.; Shamsi, R.; Perry, S. L.; Sing, C. E. Molecular Connectivity and Correlation Effects on Polymer Coacervation. *Macromolecules* **2017**, *50*, 3030–3037.

[31] Sing, C. E. Development of the modern theory of polymeric complex coacervation. *Advances in Colloid and Interface Science* **2017**, *239*, 2–16.

[32] Lee, J.; Popov, Y. O.; Fredrickson, G. H. Complex coacervation: A field theoretic simulation study of polyelectrolyte complexation. *The Journal of Chemical Physics* **2008**, *128*, 224908.

[33] Perry, S. L.; Sing, C. E. PRISM-Based Theory of Complex Coacervation: Excluded Volume versus Chain Correlation. *Macromolecules* **2015**, *48*, 5040–5053.

[34] Semenov, A. N.; Rubinstein, M. Thermoreversible Gelation in Solutions of Associative Polymers. 1. Statics. *Macromolecules* **1998**, *31*, 1373–1385.

[35] Rouse, P. E. A Theory of the Linear Viscoelastic Properties of Dilute Solutions of Coiling Polymers. *The Journal of Chemical Physics* **1953**, *21*, 1272–1280.

[36] Gennes, P. G. D. Dynamics of Entangled Polymer Solutions. I. The Rouse Model. *Macromolecules* **1976**, *9*, 587–593.

[37] Goodwin, J. W.; Hughes, R. W. *Rheology for Chemists: An Introduction*; Royal Society of Chemistry, 2008.

[38] Macosko, C. W. *Rheology: Principles, Measurements, and Applications*; Wiley-VCH, 1994.

[39] Rubinstein, M.; Colby, R. H. *Polymer Physics (Chemistry)*; Oxford University Press, 2003.

[40] Rubinstein, M.; Semenov, A. N. Dynamics of Entangled Solutions of Associating Polymers. *Macromolecules* **2001**, *34*, 1058–1068.

[41] Spruijt, E.; Sprakel, J.; Lemmers, M.; Stuart, M. A. C.; van der Gucht, J. Relaxation Dynamics at Different Time Scales in Electrostatic Complexes: Time-Salt Superposition. *Physical Review Letters* **2010**, *105*.

[42] Fares, H. M.; Wang, Q.; Yang, M.; Schlenoff, J. B. Swelling and Inflation in Polyelectrolyte Complexes. *Macromolecules* **2018**, *52*, 610–619.

[43] Fares, H. M.; Ghoussoub, Y. E.; Delgado, J. D.; Fu, J.; Urban, V. S.; Schlenoff, J. B. Scattering Neutrons along the Polyelectrolyte Complex/Coacervate Continuum. *Macromolecules* **2018**, *51*, 4945–4955.

[44] Hamad, F. G.; Chen, Q.; Colby, R. H. Linear Viscoelasticity and Swelling of Polyelectrolyte Complex Coacervates. *Macromolecules* **2018**, *51*, 5547–5555.

[45] Ali, S.; Prabhu, V. Relaxation Behavior by Time-Salt and Time-Temperature Superpositions of Polyelectrolyte Complexes from Coacervate to Precipitate. *Gels* **2018**, *4*, 11.

[46] Liu, Y.; Momani, B.; Winter, H. H.; Perry, S. L. Rheological characterization of liquid-to-solid transitions in bulk polyelectrolyte complexes. *Soft Matter* **2017**, *13*, 7332–7340.

[47] Marciel, A. B.; Srivastava, S.; Tirrell, M. V. Structure and rheology of polyelectrolyte complex coacervates. *Soft Matter* **2018**, *14*, 2454–2464.

[48] Velankar, S. S.; Giles, D. How do I know if my phase angles are correct? *Rheology Bulletin* **2007**, *76*, 8–20.

[49] Wang, J.-S.; Matyjaszewski, K. Controlled/"Living" Radical Polymerization. Halogen Atom Transfer Radical Polymerization Promoted by a Cu(I)/Cu(II) Redox Process. *Macromolecules* **1995**, *28*, 7901–7910.

[50] Lundt, B. F.; Johansen, N. L.; Vølund, A.; Markussen, J. Removal of t-Butyl and t-Butoxycarbonyl Protecting Groups with Trifluoroacetic Acid. *International Journal of Peptide and Protein Research* **2009**, *12*, 258–268.

[51] Laaser, J. E.; McGovern, M.; Jiang, Y.; Lohmann, E.; Reineke, T. M.; Morse, D. C.; Dorfman, K. D.; Lodge, T. P. Equilibration of Micelle-Polyelectrolyte Complexes: Mechanistic Differences between Static and Annealed Charge Distributions. *J. Phys. Chem. B* **2017**, *121*, 4631–4641.

[52] Carmean, R. N.; Figg, C. A.; Scheutz, G. M.; Kubo, T.; Sumerlin, B. S. Catalyst-Free Photoinduced End-Group Removal of Thiocarbonylthio Functionality. *ACS Macro Letters* **2017**, *6*, 185–189.